simATAC: A Single-cell ATAC-seq Simulation Framework

Zeinab Navidi Ghaziani[1], Lin Zhang[2] and Bo Wang[1,2,3*]

Abstract

Single-cell Assay for Transposase-Accessible Chromatin sequencing (scATAC-seq) identifies regulated chromatin accessibility modules at the single-cell resolution. Robust evaluation is critical to the development of scATAC-seq pipelines, which calls for reproducible datasets for benchmarking. We hereby present the simATAC framework, an R package that generates a scATAC-seq count matrix, highly resembling real scATAC-seq datasets in library size, sparsity, and averaged chromatin accessibility signals. simATAC deploys statistical functions derived from analyzing 90 real scATAC-seq cell groups to model read distributions. simATAC provides a robust and systematic approach to generate *in silico* scATAC-seq samples with cell labels for a comprehensive tool assessment.

Keywords: Single-cell; scATAC-seq; Simulator; Software

Background

Single-cell sequencing has revolutionized and expedited our understanding of the structure and function of cells at unprecedented resolution. This technology resolves a fundamental limitation of bulk sequencing, which averages signals over a large number of cells resulting in obscured biological heterogeneity among individual cells [1]. The assay for transposase-accessible chromatin sequencing (ATAC-seq) measures the openness of chromatin, a proxy for activity of DNA binding proteins [2–4]. Single-cell ATAC-seq (scATAC-seq) has opened up vast fields of applications, including extracting accessibility and co-accessibility patterns of genomic regions to identify cell-type-specific enhancers, chromatin heterogeneity, and transcription factor activities.

The rapid advancement of scATAC-seq technology gives rise to the development of computational tools for scATAC-seq data analysis, and the integrative analysis of transcriptomic and epigenomic profiles [5–7]. Though simulated datasets with known labels have been the most common approach to benchmark the performance of analytical pipelines, there is no existing standard practice or simulation tool available to generate synthetic scATAC-seq datasets. Furthermore, due to the sparsity and noisy nature of scATAC-seq data, generating synthetic samples that resemble real datasets is challenging. Many existing scATAC-seq analytical pipelines assessed their performance solely based on real datasets [8–14]. Some studies generated simulated data by downsampling reads from bulk ATAC-seq data [15–19] or deploying ad-hoc simulation methods [20–23]. However, these simulation methods were implemented as part of the development or evaluation of scATAC-seq pipelines and were usually incompletely documented, resulting in a lack of reproducibility.

scATAC-seq analytical pipelines usually consist of pre-processing (read quality control and alignment), core analysis (feature matrix generation) and downstream analyses (e.g. cell type clustering). A feature matrix summarizes the filtered reads from BAM files by counting the number of aligned reads that overlap within the defined genomic regions. The features represent a subset of genomic regions with specified genomic positions, nucleotide patterns, or biological functions [8, 9, 24]. A commonly used feature matrix for scATAC-seq is the peak by cell matrix that captures the highest read coverage signals from the most accessible genomic regions (peaks) obtained from bulk ATAC-seq data. However, a sufficient number of cells are required to identify such peaks, and consequently, the peak by cell feature matrix usually fails to recognize the rare cell type regulatory patterns in aggregated signals [15].

Alternatively, the bin by cell feature matrix is generated by segmenting the whole genome into uniformly-sized non-overlapping "bins" and mapping the read counts in each bin [15]. Uniform segmentation of the genome provides unbiased detection of chromatin accessibility, and enables pattern extraction from both significant and non-significant distinguishable dynamics between cells.

We hereby propose simATAC, a scATAC-seq simulation framework that generates unbiased simulated

*Correspondence: bo.wang@uhnresearch.ca
[1]Peter Munk Cardiac Centre, University Health Network, Toronto, Canada
Full list of author information is available at the end of the article

samples resembling real scATAC-seq data. Given a real scATAC-seq feature matrix as input, simATAC estimates the statistical parameters of the mapped read distribution by cell type, and generates a synthetic count array that captures the unique regulatory landscape of a group of cells with similar biological characteristics. We demonstrate that the synthetic samples generated by simATAC highly resemble real scATAC-seq datasets in library sizes, sparsity (proportion of zero entries) and averaged chromatin accessibility signals.

Results

simATAC framework

simATAC deploys statistical distributions to model the properties of a bin by cell count matrix for a group of cells with similar biological characteristics. The main modelling parameters include read coverage of cells (library size), non-zero cell proportion in each bin, and the average of counts per bin (bin mean). Bin by cell matrix quantifies the number of open chromatin read fragments falling into the non-overlapping fixed-length bins (5 kbp windows) across the whole genome. For each user-input, simATAC performs two core simulation steps: (i) estimating the model parameters based on the input bin by cell matrix, including the library sizes of the cells, the non-zero cell proportions of each bin and the read average of each bin; (ii) generating a bin by cell matrix that resembles the original input scATAC-seq data by sampling from Gaussian mixture and polynomial models with the estimated parameters. simATAC outputs a count matrix as a SCESet object [25], with additional options to convert it to other types of feature matrices. Figure 1 summarizes the simulation architecture of simATAC. The statistical modelling of simATAC is discussed in further details in the next sections and Methods.

Library size

Library size refers to the number of aligned reads per cell. simATAC models cells' log-transformed library sizes through a Gaussian mixture model (GMM) with two components whose parameters are estimated based on the user-input real scATAC-seq data. With the estimated parameters, simATAC randomly samples library sizes of C single cells based on Eq. (1).

$$\log_2(l'_i) \sim w \times \mathcal{N}(\mu_1, \sigma_1^2) + (1-w) \times \mathcal{N}(\mu_2, \sigma_2^2) \quad (1)$$

where l'_i is the simulated library size for the ith simulated single cell. See Table 1 for the detailed definition of the Gaussian mixture model parameters.

Previous studies have shown that the library sizes of cells significantly affect the identification of cell types [15–17, 19, 21]. A larger library size usually indicates higher sequencing coverage, thus providing more accurate chromatin accessibility information. Since the library sizes of scATAC-seq usually vary across different experiments, simATAC offers users the flexibility to adjust the library sizes from low to high coverage based on their needs.

Table 1 Input parameters in simATAC simulation step.

Parameter	Symbol	Description
Library size mean	μ_1, μ_2	The estimated means of two Gaussian modals of library size.
Library size standard deviation	σ_1, σ_2	The estimated standard deviations of two Gaussian modals of library size.
Library size weight	w	The estimated weight parameter of the first Gaussian modal.
Non-zero cell proportion	P	The proportion of non-zero cells in real bin by cell matrix.
Polynomial coefficients	β	The estimated coefficients of polynomial model fitted to the relation between bin non-zero cell proportions and bin means.

Bin non-zero cells proportion

Sparsity is the inherent nature of scATAC-seq data [15, 21, 26], which results in a large proportion of zero entries in the bin by cell matrix. Let $M_{j,i}$ denote the number of reads that fall into the bin j of cell i for B bins. If $M_{j,i} > 0$, then it is considered as a non-zero entry. The number of cells with non-zero entries within a bin is associated with the chromatin accessibility in the corresponding genomic region. simATAC estimates the proportion of cells with non-zero entries for the jth bin, p_j, based on the user-input real scATAC-seq bin by cell matrix, and determines if an entry's status in the simulated count matrix is zero or non-zero based on a Bernoulli distribution:

$$X_{j,i} \sim Bernoulli(p_j) \quad (2)$$

If $X_{j,i} = 1$, the read count of cell i at bin j is non-zero, i.e. $M_{j,i} > 0$. If $X_{j,i} = 0$, the read count of cell i at bin j is set to zero, i.e. $M_{j,i} = 0$. The non-zero proportion of bin j, p'_j, of the simulated bin by cell matrix is then defined as

$$p'_j = \sum_{i=1}^{C} X_{j,i}/C \quad (3)$$

Bin mean

The extent of genome accessibility leads to the variations in the number of sequenced reads falling into the

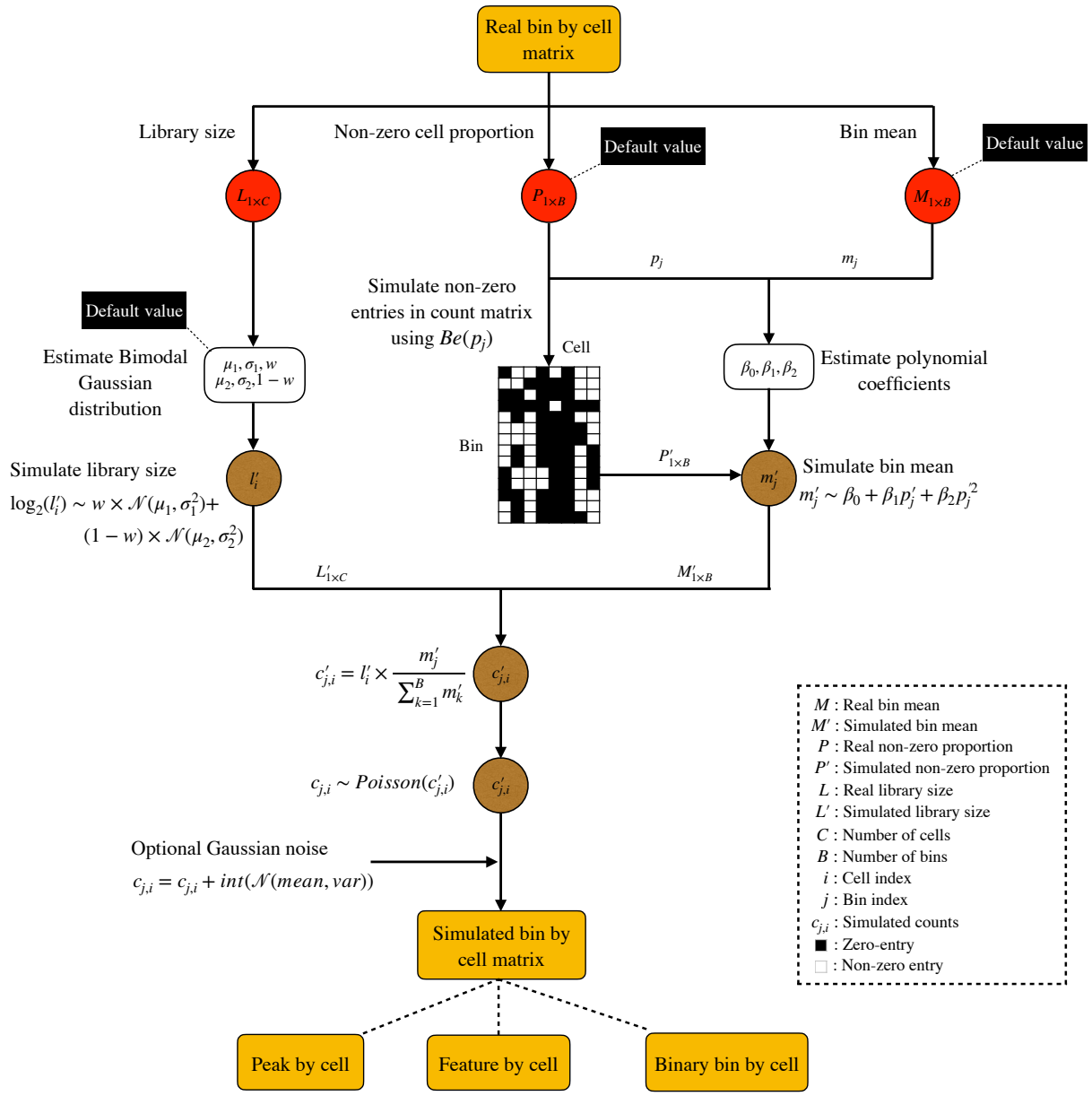

Figure 1 The simATAC simulation framework. The red circles represent values directly extracted from the user-supplied bin by cell matrix, the white squares represent estimated parameters, and the brown circles represent the simulated values. simATAC initially estimates the library sizes, the non-zero cell proportions and the bin means from the input cell group (including cells having similar biological characteristics). simATAC generates the library sizes with a Gaussian mixture distribution, the zero and non-zero status with a Bernoulli distribution, and the bin means with a polynomial regression model linking to the non-zero cell proportion. The synthetic counts are sampled from a Poisson distribution whose mean is the cell library size adjusted by the bin mean. simATAC offers an optional noise function that adjusts the synthetic counts generated from the Poisson distribution with various noise levels. Default values for the three main parameters are embedded in the simATAC framework in case no user-supplied input is given.

fixed-length bins, and consequently, the variations in the average of the reads in each bin. The more accessible a region is, the larger the bin means are, that is, the more cells with non-zero entries are mapped to that region. We observed a polynomial regression relation between the non-zero cell proportions and bin means in each cell group in the samples used for simATAC modelling. simATAC simulates the average of the read counts at bin j, m'_j, with a fitted polynomial regres-

sion model with the non-zero cell proportion, p'_j, as the explanatory variable,

$$m'_j = \beta_0 + \beta_1 p'_j + \beta_2 p'^2_j \quad (4)$$

We observed that in real scATAC-seq datasets, for each cell group, there are a few bins (on average, two bins out of hundreds of thousands of bins) with a non-zero cell proportion higher than 0.8. While the polynomial regression model is a good fit for the relation of bin means and non-zero cell proportions, it generally doesn't capture bins having a non-zero cell proportion higher than 0.8. These few bins are excluded in the polynomial modelling. However, the estimated polynomial function is used to simulate all bins through the genome.

Bin by cell count matrix

simATAC generates the final count of cell i at bin j, $c_{j,i}$, using a Poisson distribution with $c'_{j,i}$ as the mean parameter, where $c'_{j,i}$ is the library size of cell i scaled by the bin mean m'_j at bin j.

$$c'_{j,i} = l'_i \times (\frac{m'_j}{\sum_{k=1}^{B} m'_k}) \quad (5)$$

$$c_{j,i} \sim Poisson(c'_{j,i}) \quad (6)$$

To reproduce the high noise level of scATAC-seq data, simATAC offers an optional step to include additional noise by adding Gaussian noises (rounded to integer) to the final simulated counts.

$$c_{j,i} = c_{j,i} + int(\mathcal{N}(mean, sd)) \quad (7)$$

High noise level will blur the difference in the read distributions across different cell types, and mimic real sequencing artifacts. However, as the noise level increases, the distribution of the library sizes and the sparsity in the synthetic dataset may differ from the input scATAC-seq samples. The default setting of simATAC omits the optional adding noise step. However, the users have the flexibility to set their desirable noise level. Table 5 provides the recommended noise parameter settings for different noise levels.

simATAC writes the final synthesized bin by cell matrix as a SCESet object, a container for single-cell genomics data, from the SingleCellExperiment R package [25].

Simulating feature matrices

simATAC generates synthetic scATAC-seq data in the format of bin by cell, peak by cell and binarized count matrices. Peak by cell array is a commonly used representation of scATAC-seq data, where peak calling is performed on bulk samples or an aggregated scATAC-seq profile to extract genomic areas enriched with aligned reads as accessibility signal [21]. simATAC generates synthetic peak by cell count matrix with the simATACgetCellByPeak function, given a simATAC simulated object and a user-specified number of peak bins. simATAC can also generate a cell by feature matrix given an user defined list of regions of interest (in a BED format) with the simATACgetCellByRegion function. Another commonly used feature matrix format is the binary version, which is provided by simATACgetBinary function.

simATAC runtime

We assessed the performance of simATAC in terms of running time on a desktop workstation (Intel(R) Xeon(R) CPU @ 3.60GHz processor) for simulating 1,000 human cells at 5 kbp window size, which took on average 43 seconds for five different runs. Benchmark datasets' running times for estimation and simulation steps are provided separately in Additional file 1 Table S1. The running times reported in the Table S1. are for three versions of simulations runs without including Gaussian noise.

Evaluation

In this section, we demonstrate the resemblance of the simulated samples by simATAC to the input real scATAC-seq datasets. The simulated samples are compared to the real samples on the distributions of library sizes, sparsity, and bin means. We also evaluated the peak calling and clustering performance of the synthesized matrices. The evaluations are performed on each cell groups (or cell types) from the annotated benchmark scATAC-seq datasets, Buenrostro2018, Cusanovich2018, and PBMCs, representing a wide range of platforms, cell types, and species.

- The Buenrostro2018 dataset contains 1974 cells generated from the Fluidigm C1 platform. Samples are from 10 FACS-sorted cell populations from CD34+ human bone marrow, namely, hematopoietic stem cells (HSCs), multipotent progenitors (MPPs), lymphoid-primed multipotent progenitors (LMPPs), common myeloid progenitors (CMPs), granulocyte-macrophage progenitors (GMPs), megakaryocyte-erythrocyte progenitors (MEPs), common lymphoid progenitors (CLPs), plasmacytoid dendritic cells (pDCs), and monocytes (mono) [27].

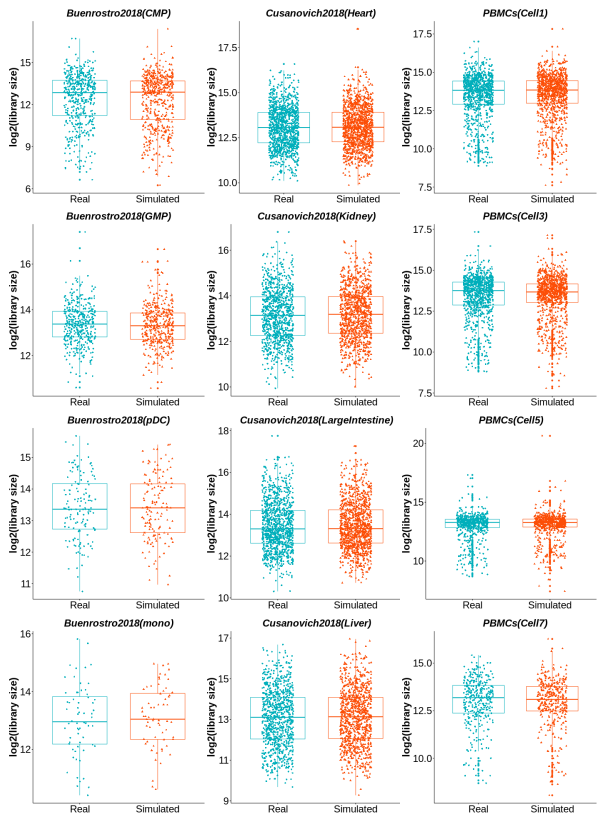

Figure 2 Comparison of the library size distribution. Library size box plots of the simulated (in orange) and real (in green) scATAC-seq data are illustrated for the three benchmarking datasets: Buenrostro2018, Cusanovich2018, and PBMCs. The library size distributions of the synthetic samples (no Gaussian noise is included) closely resemble those of the real samples.

- The Cusanovich2018 dataset is a subset of sci-ATAC-seq mouse tissues with 12178 cells from 13 different sources [21]. Sequenced cells are from bone marrow, cerebellum, heart, kidney, large intestine, liver, lung, prefrontal cortex, small intestine, spleen, testes, thymus, and whole brain, generated using a sci-ATAC-seq protocol [28].
- The PBMCs dataset is produced by the 10x Genomics Chromium (10xG) droplet-based scATAC platform and comprises 5335 cells from human peripheral blood mononuclear cells (PBMCs) [29]. There are no true cell type labels for PBMCs cells. However, we used 10x Genomics Cell Ranger ATAC's [29, 30] clustering labels as ground truth and performed simulation on each cluster. Although existing labels are not perfect, we included this data to evaluate how simATAC mimics features of a group of cells with similar biological characteristics from a droplet-based platform [21].

Table 2 Averaged Pearson correlation between the simulated and real sample bin means and the non-zero cell proportion of bins (for three simulation runs with different initial seeds).

	Correlation	
Cell type	Bin mean	Bin non-zero proportion
Buenrostro2018		
CMP	0.98	0.98
GMP	0.98	0.98
pDC	0.96	0.96
mono	0.92	0.93
Cusanovich2018		
Heart	0.95	0.96
Kidney	0.97	0.97
LargeIntestine	0.93	0.93
Liver	0.98	0.98
PBMCs		
Cell1	0.99	1
Cell3	0.99	1
Cell5	0.98	0.99
Cell7	0.99	0.99

Statistical evaluation

With each of the three real scATAC-seq datasets as benchmark data, we simulated bin by cell matrix for each cell group with the same number of cells as in the real datasets. We then compared the distribution of library sizes, bin means, and non-zero cell proportions of the simulated dataset to the real samples, by cell group. We present four cell groups from each benchmarking dataset to demonstrate the similarity.

Figure 2 depicts the box plots of library size distributions for 12 cell groups from the benchmarking datasets. The library size distributions of the simulated cells by simATAC highly resemble those of the real datasets, in the mean, the median and the quantile distribution. See Additional file 1: Fig. S1 for the complete comparisons between the real and simulated bin by cell matrices of all cell groups.

simATAC synthesized bin by cell matrices preserve the accessibility of genomic regions with matched bin mean and non-zero cell proportion patterns to the input real scATAC-seq datasets. The high correlations between the corresponding bins in the real and synthesized data (for the bin mean and non-zero cell proportion parameters) demonstrate that simATAC retains the input cells' genomic region accessibility characteristics. Table 2 summarizes the averaged Pearson correlation of each parameter based on three simulation runs. The complete version of the table, including all cell groups from the benchmarking datasets is provided in Additional file 1: Table S2.

Figure 3 illustrates the sparsity of the bin by cell matrix in 12 cell groups of the benchmark datasets, which demonstrates that the synthetic samples generated by simATAC retains the sparsity of the real sam-

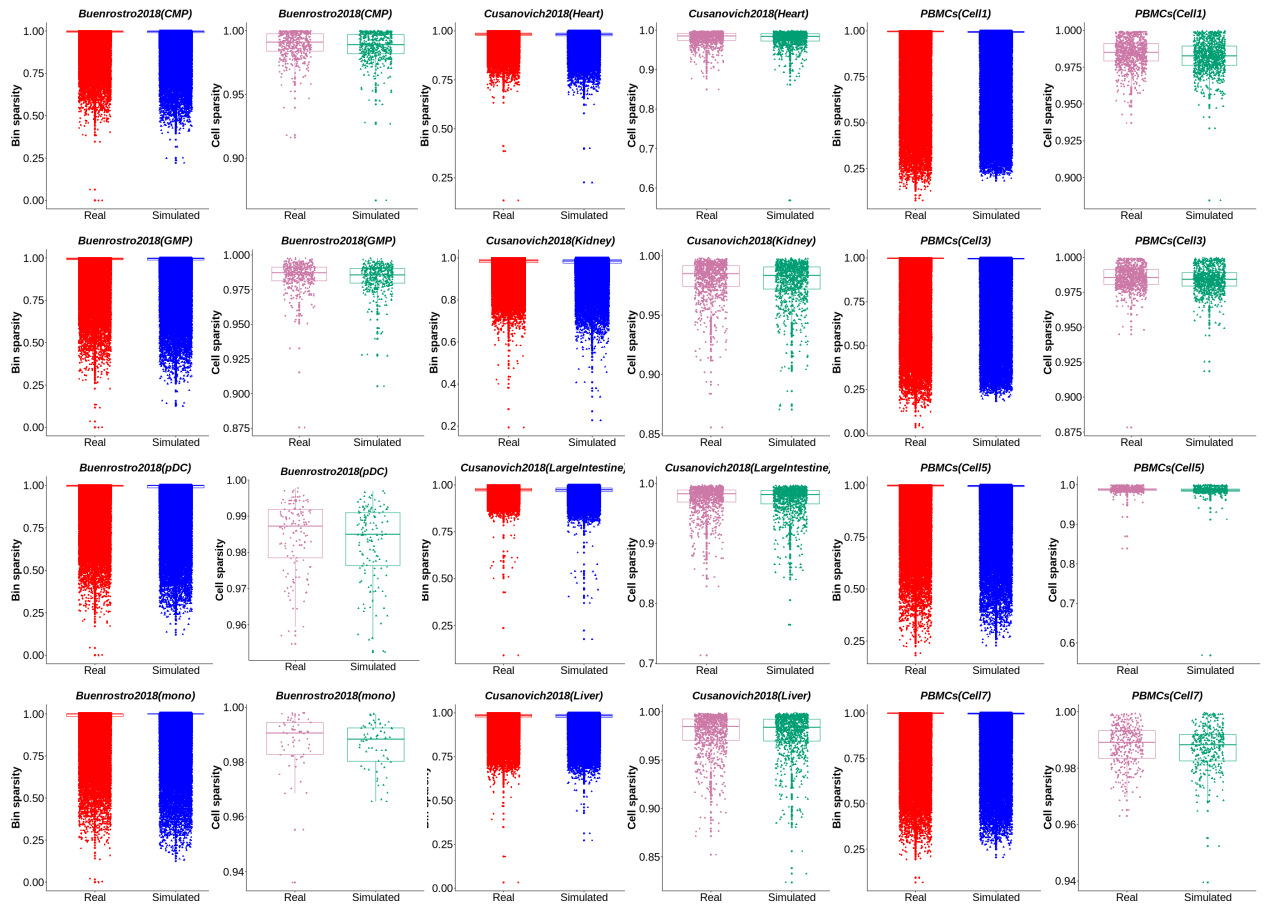

Figure 3 Comparison of the bin sparsity and cell sparsity distributions. Cell sparsity and bin sparsity box plots of the simulated (in blue for bin sparsity, and green for cell sparsity) and real (in red for bin sparsity, and purple for cell sparsity) scATAC-seq data are illustrated for the three benchmarking datasets: Buenrostro2018, Cusanovich2018, and PBMCs. The sparsity of the synthetic data generated by simATAC (no Gaussian noise is included) closely resembles that of the corresponding real scATAC-seq input data.

ples across bins and cells. See Additional file 1: Fig. S2-S3 for all cell groups comparison.

We compared simulations across metrics and datasets by calculating median absolute deviation (MAD), mean absolute error (MAE), and root mean square error (RMSE) for the main simulation parameters explained. The absolute deviation of the sorted real and sorted synthetic library size vectors, real and simulated bin means, and real and simulated bins' non-zero proportion was calculated. The MAD, MAE, and RMSE metrics for all of the three mentioned vectors of differences are shown in Table 3. Each entry in the Table 3 is averaged across all cell groups in the associated benchmarking dataset for a simulation run. We extracted these statistics to evaluate the closeness of each simulated parameter to real values. The small parameters' values being close to zero suggest that simATAC synthesizes feature matrix properties following real data patterns.

simATAC is capable of maintaining peak information from real scATAC-seq samples. For each of the benchmarking datasets, we defined three lists of peak regions and compared them:

- Pre-defined bulk peaks obtained from bulk read signals.
- Real peak bins, including 5,000 top bins with the highest bin means extracted from real data bin by cell matrix.
- Simulated peak bins, including 5,000 bins with the highest bin means from simATAC's simulated bin by cell matrix.

We first extracted the percentage of bins across the genome that are common in the extracted peak bins from the real and simulated bin by cell matrices, and then assessed the percentage of regions from pre-

Table 3 Median absolute deviation (MAD), mean absolute error (MAE), and root mean square error (RMSE) calculated for sorted real and sorted simulated library sizes, real and simulated bin means, and real and simulated non-zero cell proportions for corresponding bins. The table presents each parameter's average across all cell groups in the associated dataset.

	Buenrostro2018			Cusanovich2018			PBMCs		
	MAD	MAE	RMSE	MAD	MAE	RMSE	MAD	MAE	RMSE
Non-zero proportion	0.0005	0.0056	0.0137	0.0039	0.0057	0.0085	0.0056	0.0079	0.0126
Bin mean	0.0013	0.0078	0.5047	0.0045	0.0065	0.0298	0.0071	0.0119	0.0515
Library size	0.0735	0.0976	0.1352	0.0553	0.0692	0.0992	0.0640	0.0907	0.1407

Table 4 Peak calling analysis results. Bulk peak: peak regions obtained from bulk read signals; Real bin: 5,000 peak bins with highest bin coverage means obtained from the real bin by cell matrix; Simulated bin: 5,000 peak bins with highest bin coverage means obtained from simATAC's simulated bin by cell matrix. This table summarizes the percentage of peak regions defined in the table's rows that have overlap with the list of peak regions defined in the columns.

	Buenrostro2018			Cusanovich2018			PBMCs		
	Bulk peak	Real bin	Simulated bin	Bulk peak	Real bin	Simulated bin	Bulk peak	Real bin	Simulated bin
Bulk peak	100%	96%	96%	100%	98%	98%	100%	97%	97%
Real bin	96%	100%	94%	99%	100%	95%	96%	100%	96%
Simulated bin	96%	94%	100%	99%	95%	100%	96%	96%	100%

defined bulk peaks (downloaded for each benchmarking dataset [21]) that have an intersection with the real and simulated peak bins' coordinates. Percentage of peak bins (from both real and synthetic count arrays) with an intersection with the bulk peak regions were also extracted. The results showed that simATAC preserves the representative peak information of real scATAC-seq data similar to the peaks obtained from bulk data, and can be deployed for developing methods and downstream analysis. The details of peak analysis results and the intersection of peak regions for each pair of the defined list of peak regions are provided in Table 4.

Clustering evaluation

The ability to separate cells with similar biological characteristics from a complex cell population is one of the major evaluation aspects of many scATAC-seq analytical tools. The availability of synthetic scATAC-seq samples reflecting cell's distinct features would be remarkably useful in assessing cell clustering algorithms. Many previous studies reported close to perfect cell clustering metrics when no noise was included [15, 16, 21]. We performed clustering analysis on the synthesized bin by cell matrices generated by simATAC and compared their clustering results with those of the real datasets. We used SnapATAC [15] to pre-process and cluster the simulated bin by cell matrices as well as the real benchmarking datasets. We also simulated data with different levels of Gaussian noise parameters for this analysis, assuming the extra noise would mimic real data measurement's artifacts.

Table 5 summarizes the averaged clustering metrics, normalized mutual information (NMI), adjusted mutual information (AMI), and adjusted rand index (ARI) over three simulation runs, each with a different initial seed. The selected level of noise parameters that are provided in the Table 5 maintain read distribution reasonably close to the real data with reasonably realistic performance compared to existing ad-hoc simulation methods [15, 21] that yielded close to perfect clustering results. Further parameter plots for the simulated counts with Gaussian noise are provided in Additional file 1: Fig. S5-S10, and Table S3-S4. The closeness of the clustering performance to the real dataset is a trade-off with the closeness of the distribution of library sizes and the sparsity.

Table 5 Clustering evaluation results. The NMI, AMI, and ARI scores are the cell type clustering results using SnapATAC on the simulated and real datasets for each of Buenrostro2018, Cusanovich2018 and PBMCs datasets. Clustering results for different noise levels are also compared presented.

Mean	Standard deviation	NMI	AMI	ARI
	Buenrostro2018			
0	0	0.73	0.84	0.56
-0.3	0.3	0.72	0.83	0.55
-0.4	0.4	0.68	0.79	0.50
Real		0.57	0.65	0.40
	Cusanovich2018			
0	0	0.96	0.97	0.95
-0.3	0.3	0.79	0.85	0.70
-0.4	0.4	0.63	0.72	0.40
Real		0.41	0.47	0.22
	PBMCs			
0	0	0.80	0.88	0.74
-0.3	0.3	0.61	0.73	0.48
-0.4	0.4	0.52	0.61	0.36
Real		0.45	0.54	0.29

Discussion and conclusions

The rapid development of scATAC-seq technology has led to a surge of scATAC-seq analytical tools. However, the lack of systematic simulation frameworks hinders the consistent evaluation of the computational tools and reproducibility of the analytical results. To meet this need, we developed simATAC, a systematic scATAC-seq simulator that generates synthetic samples that closely resemble real scATAC-seq data. simATAC builds upon Gaussian mixture distribution to model cell library sizes, and polynomial regression model to represent the relationship between the average of bin counts and the non-zero cell proportions of bins. Moreover, simATAC grants users the flexibility to adjust parameters manually. simATAC generates a synthetic bin by cell matrix given a real scATAC-seq dataset as input. If there are no user-specified count matrix or parameters available, simATAC simulates synthetic bin by cell matrix using the default parameters derived from simulating the GSE99172 real scATAC-seq data. A list of estimated values for library size Gaussian mixture distribution and polynomial function parameters are provided in Additional file 2 to get the intuition of real data parameters. simATAC also offers additional functions to transform the bin by cell matrix into other feature matrices, such as peak by cell array.

We compiled and processed 90 real scATAC-seq cell groups (from eight datasets) from various sequencing technologies, platforms, species and cell types to build a generalizable framework. We demonstrated the distributions of the library sizes, non-zero cell proportions, and bin means of the simATAC synthetic datasets resembling those of the real input examples. simATAC also offers the users additional options to modify the noise levels to mimic the artifacts in real scATAC-seq data and generate samples with various difficulty levels for clustering assessment.

Quality control steps in most scATAC-seq pipelines apply filters on the raw feature matrices, such as removing cells with library sizes less than a fixed threshold, or filtering regions based on the number of mapped reads. As the denoising thresholds may affect the downstream analyses, simATAC offers users the flexibility to manually set the quality control filtration thresholds on the simulated raw count matrix and subsequent computational analyses such as binarization, dimensionality reduction, clustering, and visualization.

Cell type clustering assessments were performed on the simATAC's synthesized bin by cell matrices for the three benchmark datasets (see Table 3). The noisier the simulated samples, the more difficult the clustering task will be. We provided suggestions for the noise parameters to be used, to maintain the read distributions across cells and bins reasonably close to the real data. We consistently observed that simATAC provides reasonably realistic samples to be used for the evaluation of computational tools.

simATAC generates count matrices using a 5 kbp bin window. However, there is no standard agreement on the optimal bin size for all samples, and bin size selection induces a trade-off between the ability to capture chromatin accessibility signals and computational cost. For instance, at a 5 kbp window size, which is the recommended window size by SnapATAC for cell counts that we have compiled and used [15], each human cell spans more than 600,000 bins. Smaller bin length leads to more computational and memory costs. Notwithstanding the aforementioned challenges, we envision that simATAC will be an effective data simulation framework in the field to enable consistent benchmarking of scATAC-seq related analytical tools.

Methods

simATAC statistical modelling

We compiled and processed each of the 90 scATAC-seq cell groups as well as each of the eight datasets (considering all cell groups together) separately to model the library size parameter. We conducted the Kolmogorov-Smirnov test [31] and the Chi-squared test [32] to test the goodness of fitness of the log-transformed library sizes from the Gaussian probability distribution, using the stats and fitdistrplus R packages [33, 34]. The p-values of the goodness of fitness tests showed that non-10xG samples generally follow a Gaussian distribution. Our preliminary statistical analysis of the 10xG scATAC-seq data showed that many of them are sampled from a mixture of probability distributions. We tested the null hypothesis if the 10xG samples' library sizes are sampled from a unimodal probability distribution using Hartigan's dip test [35] from the diptest R package [36]. Most of the modelling datasets rejected the null hypothesis that the library sizes are sampled from a unimodal probability distribution at a significance level of $\alpha = 0.05$. Considering the probability density function and the cumulative distribution function plots, we modelled the log-transformed library sizes with a Gaussian mixture model with two modes and estimated the parameters using the mixtools R package [37]. Statistical parameters of the aforementioned tests for library size modelling are provided in Additional file 3.

We observed a significant difference in the distribution of library sizes between the real scATAC-seq data generated by the 10xG platform and other platforms. Library sizes of the non-10xG samples generally fit a unimodal Gaussian model, while those of the 10xG

samples fit a bimodal GMM better. simATAC simulates the library size using a bimodal GMM for samples from all platforms, and for non-10xG samples, the weight of the second Gaussian distribution can be set to zero.

To recover the scATAC-seq data sparsity, simATAC first assigns zero or non-zero labels to the bin by cell matrix using a Bernoulli distribution for each bin. The probability that a cell at bin j is non-zero is the estimated non-zero cells proportion at the corresponding bin of the input real scATAC-seq dataset.

Based on the 90 real scATAC-seq cell groups used for modelling, we observed a polynomial relationship between the non-zero cell proportions and the bin means in the normalized real bin by cell arrays. The input matrix is normalized by dividing primary counts by the cells' library size and multiplying by the median of library sizes. The quadratic relation between bin means and non-zero cell proportions in the 12 sampled cell groups of benchmarking datasets are provided in Additional file 1: Fig. S4.

simATAC estimates the regression parameters using the lm function from the stats package [33], and calculates bin means based on Eq. (4). Note that the parameters in Eq. (4) are estimated by cell types/groups, as the chromatin accessibility patterns of different cell types vary biologically. A few bins with non-zero cell proportions higher than 0.8 were filtered out in fitting the regression model in the modelling process. The average number of excluded bins is two by considering all 90 cell groups.

We assessed simATAC generated feature matrices by calculating the absolute difference between sorted real and sorted simulated library size vectors, real and simulated bin means, and non-zero cell proportion vectors of original and synthetic count matrices. We obtained MAD, MAE, and RMSE of these vectors by the following equations, where R are the real values and S are the simulated values:

$$MAD = median(|R - S|) \tag{8}$$

$$MAE = mean(|R - S|) \tag{9}$$

$$RMSE = \sqrt{mean((R - S)^2)} \tag{10}$$

Availability of data and materials

We built the simATAC statistical model and estimated the default input parameters based on 90 cell groups from eight publicly available real scATAC-seq datsets from various platforms and technologies, including Fluidigm C1, 10x Chromium, single-cell combinatorial indexing ATAC-seq (sci-ATAC-seq), and Multi-Index single cell ATAC-seq (MI-ATAC) to ensure a generalizable simulation framework. The datasets supporting the modelling and evaluation of this article are all available publicly. All datasets used in this study are available from NIH GEO: (1) 63 10xG sample groups from GSE129785 [29], (2) GSE99172 [8], (3) GSE74310 [38], (4) GSE65360 [39], (5) GSE68103 (GSM1647122) [12], (6) GSE68103 (GSM1647123) [12], (7) GSE112091 (series GSE112245) [40], and (8) GSE100033 (GSM2668124) [41].

The datasets used for assessing and supporting the findings of this study are available publicly: (1) a dataset of sorted human bone marrow hematopoietic cells (Buenrostro2018) [27], (2) a subset of 13 sci-ATAC-seq adult mouse tissues (Cusanovich2018) [26, 28] provided by [21], and (3) human hematopoiesis II (PBMCs) [29] provided by 10xG, which are described in the Evaluation section in detail. The detailed information of all samples with cell groups and numbers are provided in the Additional file 1: Table S5.

We used SnapTools and SnapATAC softwares for data preprocessing, generating raw bin by cell matrices, and clustering analysis:

- Project name: SnapTools, SnapATAC
- Project home page: https://github.com/r3fang/SnapATAC
- Archived version: https://doi.org/10.1101/615179
- Operating system(s): Linux/Unix
- Programming language: Python and R
- Other requirements: Python ($\geq$ 2.7 & $<$ 3.0) (SnapTools) (highly recommanded for 2.7); R ($\geq$ 3.4.0 & $<$ 3.6.0) (SnapATAC) (3.6 does not work for rhdf5 package);
- License: GPLv3
- Any restrictions to use by non-academics: -

Dataset preprocessing

The raw FASTQ or BAM files were downloaded from the links provided and bin by cell matrices used in simATAC development were generated using the SnapTools [15, 42]. SnapTools is a Python module that preprocesses scATAC-seq data. SnapTools aligns raw FASTQ files to the GRCh38 or the MM10 reference genomes using the Burrows-Wheeler aligner. Reads that were properly paired according to the SAM flag value, uniquely mapped with mapping quality > 30, and had a length less than 1,000 base pairs were filtered for further analyses. SnapTools groups the reads with the same barcode and removes PCR duplicate reads in each group. SnapTools outputs a .snap file, an hdf5 file that stores the input scATAC-seq data, including cell by bin matrix used in the development and analyses of simATAC modelling [15] [1]. For 10xG sam-

[1] https://github.com/r3fang/SnapATAC/wiki/FAQs#CEMBA_snap

ples [2], we started from the fragment.tsv files provided by 10x website [3], which is a barcoded and aligned fragment file processed, with an implemented option by SnapTools for 10xG samples. The rest of the samples were processed from FASTQ or provided BAM files, and unique randomly generated barcodes were added to the samples that did not have barcodes themselves.

The code and dataset files used for benchmarking are available at https://github.com/bowang-lab/simATAC.

Declarations

Competing interests

The authors declare that they have no competing interests.

Availability of data and materials

The datasets analyzed during the current study are available from the repositories specified in the methods. The code used to analyze them is available under an GPLv3 license from the repository for this paper https://github.com/bowang-lab/simATAC. Copies of the benchmarking datasets are also provided in this repository. The simATAC package, which is the version used in this paper, is available on Github (https://github.com/bowang-lab/simATAC) under a GPLv3 license.

Author's contributions

ZN developed the software and performed the analyses. LZ contributed to the statistical analyses and writing the manuscript. BW oversaw all aspects of the project. All authors contributed to drafting the manuscript. All authors read and approved the final manuscript.

Acknowledgements

We would like to thank our lab mates Chloe Wang, Hassaan Maan, Mehran Karimzadeh, Rex Ma, and Ronald Xie for their helpful comments on the manuscript.

Funding

B.W. is partly supported by CIFAR AI Chair Programs.

Consent for publication

Not applicable.

Ethics approval and consent to participate

Not applicable.

Author details

[1]Peter Munk Cardiac Centre, University Health Network, Toronto, Canada. [2]University of Toronto, Toronto, Canada. [3]Vector Institute, Toronto, Canada.

References

1. Olsen, T.K., Baryawno, N.: Introduction to Single-Cell RNA Sequencing. Current Protocols in Molecular Biology (2018). doi:10.1002/cpmb.57
2. Thurman, R.E., Rynes, E., Humbert, R., Vierstra, J., Maurano, M.T., Haugen, E., Sheffield, N.C., Stergachis, A.B., Wang, H., Vernot, B., Garg, K., John, S., Sandstrom, R., Bates, D., Boatman, L., Canfield, T.K., Diegel, M., Dunn, D., Ebersol, A.K., Frum, T., Giste, E., Johnson, A.K., Johnson, E.M., Kutyavin, T., Lajoie, B., Lee, B.K., Lee, K., London, D., Lotakis, D., Neph, S., Neri, F., Nguyen, E.D., Qu, H., Reynolds, A.P., Roach, V., Safi, A., Sanchez, M.E., Sanyal, A., Shafer, A., Simon, J.M., Song, L., Vong, S., Weaver, M., Yan, Y., Zhang, Z., Zhang, Z., Lenhard, B., Tewari, M., Dorschner, M.O., Hansen, R.S., Navas, P.A., Stamatoyannopoulos, G., Iyer, V.R., Lieb, J.D., Sunyaev, S.R., Akey, J.M., Sabo, P.J., Kaul, R., Furey, T.S., Dekker, J., Crawford, G.E., Stamatoyannopoulos, J.A.: The accessible chromatin landscape of the human genome. Nature (2012). doi:10.1038/nature11232
3. Stergachis, A.B., Neph, S., Reynolds, A., Humbert, R., Miller, B., Paige, S.L., Vernot, B., Cheng, J.B., Thurman, R.E., Sandstrom, R., Haugen, E., Heimfeld, S., Murry, C.E., Akey, J.M., Stamatoyannopoulos, J.A.: Developmental fate and cellular maturity encoded in human regulatory DNA landscapes. Cell (2013). doi:10.1016/j.cell.2013.07.020
4. Buenrostro, J.D., Wu, B., Chang, H.Y., Greenleaf, W.J.: ATAC-seq: A method for assaying chromatin accessibility genome-wide. Current Protocols in Molecular Biology (2015). doi:10.1002/0471142727.mb2129s109
5. Jin, S., Zhang, L., Nie, Q.: scAI: an unsupervised approach for the integrative analysis of parallel single-cell transcriptomic and epigenomic profiles. Genome biology (2020). doi:10.1186/s13059-020-1932-8
6. Stuart, T., Butler, A., Hoffman, P., Hafemeister, C., Papalexi, E., Mauck, W.M., Hao, Y., Stoeckius, M., Smibert, P., Satija, R.: Comprehensive Integration of Single-Cell Data. Cell (2019). doi:10.1016/j.cell.2019.05.031
7. Butler, A., Hoffman, P., Smibert, P., Papalexi, E., Satija, R.: Integrating single-cell transcriptomic data across different conditions, technologies, and species. Nature Biotechnology (2018). doi:10.1038/nbt.4096
8. Schep, A.N., Wu, B., Buenrostro, J.D., Greenleaf, W.J.: ChromVAR: Inferring transcription-factor-associated accessibility from single-cell epigenomic data. Nature Methods (2017). doi:10.1038/nmeth.4401
9. de Boer, C.G., Regev, A.: BROCKMAN: Deciphering variance in epigenomic regulators by k-mer factorization. BMC Bioinformatics (2018). doi:10.1186/s12859-018-2255-6
10. Ji, Z., Zhou, W., Ji, H.: Single-cell regulome data analysis by SCRAT. Bioinformatics (2017). doi:10.1093/bioinformatics/btx315
11. Pliner, H.A., Packer, J.S., McFaline-Figueroa, J.L., Cusanovich, D.A., Daza, R.M., Aghamirzaie, D., Srivatsan, S., Qiu, X., Jackson, D., Minkina, A., Adey, A.C., Steemers, F.J., Shendure, J., Trapnell, C.: Cicero Predicts cis-Regulatory DNA Interactions from Single-Cell Chromatin Accessibility Data. Molecular Cell (2018). doi:10.1016/j.molcel.2018.06.044
12. Cusanovich, D.A., Daza, R., Adey, A., Pliner, H.A., Christiansen, L., Gunderson, K.L., Steemers, F.J., Trapnell, C., Shendure, J.: Multiplex single-cell profiling of chromatin accessibility by combinatorial cellular indexing. Science (2015). doi:10.1126/science.aab1601
13. Zamanighomi, M., Lin, Z., Daley, T., Chen, X., Duren, Z., Schep, A., Greenleaf, W.J., Wong, W.H.: Unsupervised clustering and epigenetic classification of single cells. Nature Communications (2018). doi:10.1038/s41467-018-04629-3
14. Baker, S.M., Rogerson, C., Hayes, A., Sharrocks, A.D., Rattray, M.: Classifying cells with Scasat, a single-cell ATAC-seq analysis tool. Nucleic acids research (2019). doi:10.1093/nar/gky950
15. Fang, R., Preissl, S., Hou, X., Lucero, J., Wang, X., Motamedi, A., Shiau, A.K., Mukamel, E.A., Zhang, Y., Behrens, M.M., Ecker, J., Ren, B.: Fast and Accurate Clustering of Single Cell Epigenomes Reveals Cis-Regulatory Elements in Rare Cell Types. bioRxiv (2019). doi:10.1101/615179
16. Bravo González-Blas, C., Minnoye, L., Papasokrati, D., Aibar, S., Hulselmans, G., Christiaens, V., Davie, K., Wouters, J., Aerts, S.: cisTopic: cis-regulatory topic modeling on single-cell ATAC-seq data. Nature Methods (2019). doi:10.1038/s41592-019-0367-1
17. Urrutia, E., Chen, L., Zhou, H., Jiang, Y.: Destin: toolkit for single-cell analysis of chromatin accessibility. Bioinformatics **35**(19), 3818–3820 (2019). doi:10.1093/bioinformatics/btz141. https://academic.oup.com/bioinformatics/article-pdf/35/19/3818/30061708/btz141.pdf
18. Li, B., Li, Y., Li, K., Zhu, L., Yu, Q., Cai, P., Fang, J., Zhang, W., Du, P., Jiang, C., Lin, J., Qu, K.: APEC: an accesson-based method for single-cell chromatin accessibility analysis. Genome biology (2020). doi:10.1186/s13059-020-02034-y
19. Zhao, C., Hu, S., Huo, X., Zhang, Y.: Dr.seq2: A quality control and analysis pipeline for parallel single cell transcriptome and epigenome data. PLoS ONE (2017). doi:10.1371/journal.pone.0180583
20. Xiong, L., Xu, K., Tian, K., Shao, Y., Tang, L., Gao, G., Zhang, M., Jiang, T., Zhang, Q.C.: SCALE method for single-cell ATAC-seq analysis via latent feature extraction. Nature Communications (2019).

[2]GSE129785

[3]https://support.10xgenomics.com/single-cell-atac/software/pipelines/latest/output/fragments

doi:10.1038/s41467-019-12630-7
21. Chen, H., Lareau, C., Andreani, T., Vinyard, M.E., Garcia, S.P., Clement, K., Andrade-Navarro, M.A., Buenrostro, J.D., Pinello, L.: Assessment of computational methods for the analysis of single-cell ATAC-seq data (2019). doi:10.1101/739011. https://doi.org/10.1101/739011
22. Yu, W., Uzun, Y., Zhu, Q., Chen, C., Tan, K.: scATAC-pro: a comprehensive workbench for single-cell chromatin accessibility sequencing data. Genome biology (2020). doi:10.1186/s13059-020-02008-0
23. Duren, Z., Chen, X., Zamanighomi, M., Zeng, W., Satpathy, A.T., Chang, H.Y., Wang, Y., Wong, W.H.: Integrative analysis of single-cell genomics data by coupled nonnegative matrix factorizations. Proceedings of the National Academy of Sciences of the United States of America (2018). doi:10.1073/pnas.1805681115
24. Li, Z., Schulz, M.H., Look, T., Begemann, M., Zenke, M., Costa, I.G.: Identification of transcription factor binding sites using ATAC-seq. Genome Biology (2019). doi:10.1186/s13059-019-1642-2
25. Lun, A., Risso, D.: SingleCellExperiment: S4 Classes for Single Cell Data. (2019). R package version 1.4.1
26. Xiong, L., Xu, K., Tian, K., Shao, Y., Tang, L., Gao, G., Zhang, M., Jiang, T., Zhang, Q.C.: SCALE method for single-cell ATAC-seq analysis via latent feature extraction. Nature Communications (2019). doi:10.1038/s41467-019-12630-7
27. Buenrostro, J.D., Corces, M.R., Lareau, C.A., Wu, B., Schep, A.N., Aryee, M.J., Majeti, R., Chang, H.Y., Greenleaf, W.J.: Integrated Single-Cell Analysis Maps the Continuous Regulatory Landscape of Human Hematopoietic Differentiation. Cell (2018). doi:10.1016/j.cell.2018.03.074
28. Cusanovich, D.A., Hill, A.J., Aghamirzaie, D., Daza, R.M., Pliner, H.A., Berletch, J.B., Filippova, G.N., Huang, X., Christiansen, L., DeWitt, W.S., Lee, C., Regalado, S.G., Read, D.F., Steemers, F.J., Disteche, C.M., Trapnell, C., Shendure, J.: A Single-Cell Atlas of In Vivo Mammalian Chromatin Accessibility. Cell (2018). doi:10.1016/j.cell.2018.06.052
29. Satpathy, A.T., Granja, J.M., Yost, K.E., Qi, Y., Meschi, F., McDermott, G.P., Olsen, B.N., Mumbach, M.R., Pierce, S.E., Corces, M.R., Shah, P., Bell, J.C., Jhutty, D., Nemec, C.M., Wang, J., Wang, L., Yin, Y., Giresi, P.G., Chang, A.L.S., Zheng, G.X.Y., Greenleaf, W.J., Chang, H.Y.: Massively parallel single-cell chromatin landscapes of human immune cell development and intratumoral T cell exhaustion. Nature Biotechnology **37**(8), 925–936 (2019). doi:10.1038/s41587-019-0206-z
30. Cell Ranger ATAC. https://support.10xgenomics.com/single-cell-atac/software/pipelines/latest/what-is-cell-ranger-atac
31. Hassani, H., Silva, E.S.: A Kolmogorov-Smirnov based test for comparing the predictive accuracy of two sets of forecasts. Econometrics (2015). doi:10.3390/econometrics3030590
32. F.R.S., K.P.: X. on the criterion that a given system of deviations from the probable in the case of a correlated system of variables is such that it can be reasonably supposed to have arisen from random sampling. The London, Edinburgh, and Dublin Philosophical Magazine and Journal of Science **50**(302), 157–175 (1900). doi:10.1080/14786440009463897. https://doi.org/10.1080/14786440009463897
33. R Core Team: R: A Language and Environment for Statistical Computing. R Foundation for Statistical Computing, Vienna, Austria (2019). R Foundation for Statistical Computing. https://www.R-project.org/
34. Delignette-Muller, M.L., Dutang, C.: fitdistrplus: An R package for fitting distributions. Journal of Statistical Software **64**(4), 1–34 (2015)
35. Hartigan, J.A., Hartigan, P.M.: The Dip Test of Unimodality. The Annals of Statistics (1985). doi:10.1214/aos/1176346577
36. Maechler, M.: Diptest: Hartigan's Dip Test Statistic for Unimodality - Corrected. (2016). R package version 0.75-7. https://CRAN.R-project.org/package=diptest
37. Benaglia, T., Chauveau, D., Hunter, D.R., Young, D.: mixtools: An R package for analyzing finite mixture models. Journal of Statistical Software **32**(6), 1–29 (2009)
38. Corces, M.R., Buenrostro, J.D., Wu, B., Greenside, P.G., Chan, S.M., Koenig, J.L., Snyder, M.P., Pritchard, J.K., Kundaje, A., Greenleaf, W.J., Majeti, R., Chang, H.Y.: Lineage-specific and single-cell chromatin accessibility charts human hematopoiesis and leukemia evolution. Nature Genetics (2016). doi:10.1038/ng.3646
39. Buenrostro, J.D., Wu, B., Litzenburger, U.M., Ruff, D., Gonzales, M.L., Snyder, M.P., Chang, H.Y., Greenleaf, W.J.: Single-cell chromatin accessibility reveals principles of regulatory variation. Nature (2015). doi:10.1038/nature14590
40. Chen, X., Litzenburger, U.M., Wei, Y., Schep, A.N., LaGory, E.L., Choudhry, H., Giaccia, A.J., Greenleaf, W.J., Chang, H.Y.: Joint single-cell DNA accessibility and protein epitope profiling reveals environmental regulation of epigenomic heterogeneity. Nature Communications (2018). doi:10.1038/s41467-018-07115-y
41. Preissl, S., Fang, R., Huang, H., Zhao, Y., Raviram, R., Gorkin, D.U., Zhang, Y., Sos, B.C., Afzal, V., Dickel, D.E., Kuan, S., Visel, A., Pennacchio, L.A., Zhang, K., Ren, B.: Single-nucleus analysis of accessible chromatin in developing mouse forebrain reveals cell-type-specific transcriptional regulation. Nature Neuroscience (2018). doi:10.1038/s41593-018-0079-3
42. Fang, R.: SnapATAC: Single Nucleus Analysis Package for ATAC-Seq. (2019). R package version 1.0.0. https://github.com/r3fang/SnapATAC

Additional Files

Additional file 1 — Figure S1-S10, Table S1-S5
Figures of parameter comparison for cell groups that are not provided in the main manuscript, comparison of real and simulated parameters' polynomial relation for 12 sample cell groups, parameter plots for simATAC simulated data with noise, table of benchmarking datasets' simulation time, table of correlation, and table of all datasets' detailed information (provided in PDF format).

Additional file 2
Table of estimated values for Gaussian mixture model and polynomial function parameters obtained for benchmarking cell groups (provided in XLSX format).

Additional file 3
Table of statistical analysis parameters of simATAC library size modelling (provided in XLSX format).